A Robust Indoor Positioning System for Heterogeneous Mobile Devices

Han Zou, Baoqi Huang, *Member, IEEE,* Xiaoxuan Lu, Hao Jiang, *Member, IEEE,* and Lihua Xie, *Fellow, IEEE*

***Abstract*—Indoor Positioning System (IPS) has become one of the most attractive research fields due to the increasing demands on Location Based Services (LBSs) in indoor environments. Various IPSs have been developed under different circumstances, and most of them adopt the fingerprinting technique to mitigate pervasive indoor multipath effects. However, the performance of the fingerprinting technique severely suffers from device heterogeneity existing across commercial off-the-shelf mobile devices (e.g. smart phones, tablet computers, etc.) and indoor environmental changes (e.g. the number, distribution and activities of people, the placement of furniture, etc.). In this paper, we transform the Received Signal Strength (RSS) to a standardized location fingerprint based on the Procrustes analysis, and introduce a similarity metric, termed Signal Tendency Index (STI), for matching standardized fingerprints. An analysis on the capability of the proposed STI in handling device heterogeneity and environmental changes is presented. We further develop a robust and precise IPS by integrating the merits of both the STI and Weighted Extreme Learning Machine (WELM). Finally, extensive experiments are carried out and a performance comparison with existing solutions verifies the superiority of the proposed IPS in terms of robustness to device heterogeneity.**

***Index Terms*—Indoor Positioning System (IPS); Device Heterogeneity; Procrustes Analysis; Weighted Extreme Learning Machine.**

I. Introduction

THE explosive proliferation of mobile devices and the popularity of social networks have spurred extensive demands on Location Based Services (LBSs) in recent decades. The GPS (Global Positioning System) has been widely used in outdoor positioning, but is incapable of providing positioning services with sufficient localization accuracy in indoor environments due to the lack of line of sight (LoS) transmission channels between satellites and an indoor receiver [1]. Therefore, great efforts have been devoted to developing Indoor Positioning Systems (IPSs) so as to enable reliable and precise indoor positioning and navigation in the past two decades [2]–[5]. Unlike other wireless technologies requiring the deployment of extra infrastructures, the existing IEEE 802.11 (WiFi) network infrastructures, such as WiFi routers, have been widely available in large numbers of commercial and residential buildings, and more importantly, nearly every existing commercial mobile device is WiFi enabled. As such, WiFi based IPS has become the primary alternative to GPS for indoor positioning.

Though received signal strength (RSS) is related to the distance of a transmitter-receiver pair, it is hard to characterize the relationship by using explicit formulas. Hence, the WiFi fingerprinting approach [6]–[9] is proposed by leveraging RSS as location fingerprints, which involves two phases: an offline training phase and an online localization phase. In the offline training phase, a site survey is performed to record the fingerprints (i.e. WiFi RSS values) from multiple access points (APs) at some known locations, based on which a fingerprint database (radio map) is produced. In the online localization phase, when a device sends a location query containing its current WiFi RSS values from multiple APs, its location will be estimated using the fingerprint database.

It is acknowledged that the fingerprinting approach results in high localization accuracy provided that the testing device is the same as the reference device and under the same environment, but can be severely degenerated for heterogeneous devices [10]. Due to the proliferation of various types and brands of mobile devices, it is indispensable and urgent to develop a robust location fingerprinting technique so as to provide accurate, reliable and fast indoor positioning services for heterogeneous devices. In addition, indoor environments often change over time, and consequently, the fingerprint database built in the offline phase can deviate from the truth during the online phase, such that the robustness of the fingerprinting-based IPS is inevitably affected.

In the literature, different methods have been developed for the treatment of device heterogeneity [10]–[18]. However, these existing methods require laborious manual adjustment of RSS values during the offline stage when the testing device and the reference device are distinct. Furthermore, only limited existing work is related to mitigating the influences of indoor environmental changes; for example, the crowdsourcing based IPS (e.g. [19]–[23]) is able to partially adapt to indoor environmental changes for the sake of fingerprints crowdsourced at different times, but such fingerprints suffer from low accuracy. In order to address robustness issues with respect to both the device heterogeneity and environmental dynamics, in this

This work is funded by the Republic of Singapore National Research Foundation (NRF) through a grant to the Berkeley Education Alliance for Research in Singapore (BEARS) for the Singapore-Berkeley Building Efficiency and Sustainability in the Tropics (SinBerBEST) Program. BEARS has been established by the University of California, Berkeley as a center for intellectual excellence in research and education in Singapore. The work is also partially funded by Republic of Singapore NRF under grant NRF2013EWT-EIRP04-012 and NRF2011NRF-CRP001-090. The research of B. Huang is supported in part by the National Natural Science Foundation of China under Grants 61461037 and 41401519, and the Natural Science Foundation of Inner Mongolia Autonomous Region of China under Grant 2014MS0604.

H. Zou, X. Lu, H. Jiang and L. Xie are with the School of Electrical and Electronics Engineering, Nanyang Technological University, Singapore (e-mail: (zouhan, xlu010, jiangh, elhxie)@ntu.edu.sg).

B. Huang (Corresponding Author) is with the College of Computer Science, Inner Mongolia University, Hohhot 010021, China, and was with the School of Electrical and Electronic Engineering, Nanyang Technological University, Singapore 639798 (e-mail: cshbq@imu.edu.cn).

paper, we propose to standardize WiFi fingerprints based on a statistical shape analysis method (i.e. Procrustes analysis) [24], and define Signal Tendency Index (STI) to measure the similarity between such standardized location fingerprints. A theoretical analysis indicates that STI, which is convenient to be derived in an online fashion, displays outstanding tolerance of device heterogeneity and indoor environmental changes. More importantly, STI can be straightforwardly integrated with existing WiFi localization schemes, such as KNN based schemes [6], [7], [25], machine learning based schemes [26], [27] and so on, to improve their robustness. Furthermore, considering the fact that ELM (Extreme Learning Machine) [26], [27] provides good generalization performance at an extremely fast learning speed, we combine the weighted version of ELM, termed WELM [28], and STI to develop an efficient and robust IPS, termed STI-WELM. To be specific, STI-WELM employs STI to standardize RSS values measured by online testing devices and collected by the reference device during the offline site survey. By leveraging our proposed weighting scheme, which considers the relative importance of each RSS sample according to its corresponding STI value, a weight matrix for STI-WELM offline training is constructed, which establishes a STI-WELM model with high robustness. Extensive experiments have been conducted, and the results show that the proposed STI-WELM scheme provides more reliable and precise localization accuracy than other approaches.

To sum up, the main contribution of the paper lies in the development of a new methodology for handling device heterogeneity and environmental dynamics by standardizing RSS values. A robust indoor localization algorithm: STI-WELM is developed by integrating the merits of both STI and WELM. Both theoretical analysis and extensive experiments are carried out to verify the capability and demonstrate the superiority of the proposed method.

The rest of the paper is organized as follows. The related work is briefly reviewed in Section II. Section III introduces STI and then provides a theoretical and experimental analysis to demonstrate its capability and usefulness in handling device heterogeneity and environmental dynamics. Section IV presents the proposed STI-WELM algorithm. In Section V, our experimental testbed and data collection procedure are elaborated at first, and then experimental results and performance evaluation of the proposed scheme are reported. We conclude this paper in Section VI.

II. Related Work

In this section, we shall present a brief overview on fingerprinting-based IPS and introduce the device heterogeneity issue in indoor localization.

A. Fingerprinting-based IPS

The basic idea of the fingerprinting technique is to fingerprint each location of interest and locate a mobile device using nearest neighbor matching. Miscellaneous techniques have been incorporated into the fingerprinting approach. For instance, the Bayesian Inference is exploited in [29] to improve the localization accuracy. Some deterministic inference techniques such as the K nearest neighbor (KNN) inference have also been used to estimate locations of occupants [6], [7], [25]. Furthermore, other approaches adopt machine learning methods, including neural networks [30], Back-propagation (BP) [3], support vector machine for regression (SVR) [31], compressed sensing [32], factor graphs [33], kernel estimation [11], [34], [35] and etc. It is noteworthy that one of the machine learning algorithms, extreme learning machine (ELM), has attracted significant attention in recent years due to its fast learning and easy implementation [26], [27]. In [5], [36], an RFID-based IPS adopting the ELM has been reported to deliver a better performance in terms of both efficiency and localization accuracy. In addition, online sequential extreme learning machine (OS-ELM), which can adapt to various environmental dynamics by its online sequential learning ability, can provide higher localization accuracy consistently than traditional approaches [37].

B. Device Heterogeneity

The device heterogeneity issue occurs when the clients' mobile devices (testing devices) are different from the reference device (device utilized for the offline site survey). Due to the heterogeneous factors of mobile devices, including distinct WiFi chipsets, WiFi antennas, hardware drivers, encapsulation materials, and even operating systems [17], [38], RSS detected by heterogeneous devices at the same location usually has different mean values, and will be translated into different physical locations by the traditional WiFi RSS fingerprinting technique, with the result that localization accuracy is severely degraded [10], [11]. To handle the device heterogeneity issue encountered by the WiFi fingerprinting-based IPS, different schemes were proposed [10]–[18], [39].

One effective but time-consuming solution is to manually adjust RSS values for distinct testing devices by a linear transformation method [11], [13], [14]. Various transformation functions, such as Kullback-Leibler divergence [11], time-space sampling [13], Gaussian fit sensor model [14], have been leveraged. The main drawback of this approach is that it requires the types of the heterogeneous mobile devices be known in advance such that an offline regression procedure can be conducted to derive pairwise linear relationships. This imposes strict limitations on widespread applications involving a mass of new and unknown mobile devices. Moreover, as pointed out in [11], the linear transformation could not satisfactorily resolve the device heterogeneity issue since the simple linear relationship cannot effectively characterize the difference across mobile devices.

Some calibration-free methods were proposed in [16], [17] to avert the tedious manual RSS calibration procedure for each testing device. Collaborative mapping was employed to estimate a linear mapping function by training online measured RSS values [16]. Unsupervised learning methods such as online regression and expectation-maximization have been leveraged to learn the mapping function [17]. Nevertheless, these methods rely on time-consuming online processing to guarantee localization accuracy. Another way to address the device heterogeneity issue is to define and use

alternative location fingerprint instead of absolute RSS values. For instance, signal strength difference (SSD), which leverages the difference of RSS values as a location fingerprint, was proposed in [10], [18]. The main drawback of SSD is the effect of shadowing variation and reduced number of RSS fingerprint vectors. On the other hand, hyperbolic location fingerprinting (HLF) employs the RSS ratio between a pair of APs as a location fingerprint [15], [39]. In [10], [12], the experimental results demonstrated that SSD is better than HLF for heterogeneous devices as a location fingerprint.

III. Standardizing WiFi Fingerprints Based on the Procrustes Analysis Method

In this section, we shall introduce a technique to standardize WiFi fingerprints to improve the robustness of the fingerprinting-based IPS.

A. Definitions

During the offline site survey phase, only one mobile device (MD) is required as a reference device (RD), and the RSS fingerprints from all the APs at each reference point (RP) are collected and stored in the fingerprint database. Suppose that there are m RPs and n APs in total, and at each RP, p RSS fingerprints are collected by the RD from n APs. The mean RSS vector at the i-th RP (denoted by RP_i) is defined as RDS_i of order n, in which the j-th element is the mean RSS value collected at RP_i from the j-th AP (denoted AP_j) during a period of time. In the case when the location of RP_i is out of the detectable range of AP_j, we let the corresponding mean RSS be the minimum detectable RSS value, i.e. -100 dBm.

During the online phase, the RSS values measured by a testing device (TD) from all the APs are denoted by a vector $TDS = [P_1, ...P_j, ..., P_n]$, in which P_j is the mean RSS value collected over a period of time from AP_j. Likewise, the minimum detectable RSS value of any TD is $-100dBm$.

B. Experimental Analysis

In order to better understand device heterogeneity and grasp the key features of RSS values from heterogeneous devices, we conduct an experiment using five different mobile devices, including iPhone 5S, iPad Air, Nokia E71, Samsung GT-P1000 Galaxy Tab and Fujitsu LifeBook T4220. In a typical indoor environment (The Internet of Things Laboratory in School of Electrical and Electronic Engineering, Nanyang Technological University), 60 RSS samples are measured within one minute for each of the five mobile devices at the same location with respect to 8 WiFi APs installed at different locations. As can be seen in Fig. 1, each curve connects the average RSS values between one device and 8 APs. The RSS values associated with different mobile devices are significantly different, which verifies the effect of device heterogeneity. It is also conceivable that, if one device (say Nokia E71) is employed as a reference device in the offline site survey to create the WiFi fingerprint database and another device (say iPad Air) is considered to be positioned in the online phase, then the fingerprint matching result (say using Euclidean distance) will return the true location or any nearby location at an extremely low probability due to the obvious gap between any pair of the curves. Hence, the indoor localization accuracy will be remarkably degraded.

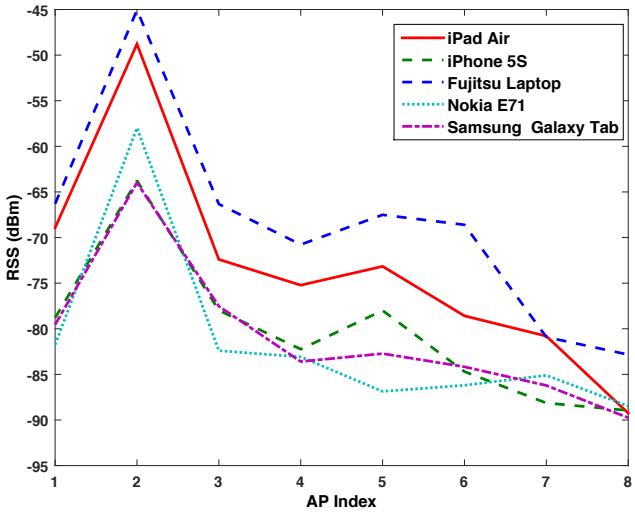

Fig. 1. WiFi RSS values measured by different mobile devices at the same location.

It is notable that, although the differences exist between any pair of curves from different devices, the shapes of the curves display certain similarities, as shown in Fig. 1; in other words, one curve can be roughly recovered from another one via translation and scale operations. This observation motivates us that, instead of matching RSS fingerprints directly, a better performance may be obtainable by comparing the shapes of the curves associated with different devices. Intuitively, since shape comparison is immune to rotation, translation and scale, the negative effect of device heterogeneity can be mitigated.

C. Standardizing RSS Fingerprints

Based on the analysis in the previous subsection, we adopt the most well-known and popular ordinary Procrustes analysis (PA) method [24] in the field of statistical shape analysis for the purpose of shape comparison. To compare the shapes of two or more objects, the PA method optimally "superimposes" all the given objects by optimally translating, uniformly scaling and rotating them. In our case, a fingerprint (which is represented by a RSS vector, e.g. TDS) denotes an object, but due to the fact that such a fingerprint can be regarded as a one-dimensional object, only the translation and uniformly scaling operations of the ordinary PA method are involved.

Given a RSS vector of a TD, namely TDS, the translation step of the ordinary PA method will produce

$$P_1 - \overline{TDS}, P_2 - \overline{TDS}, ..., P_n - \overline{TDS} \tag{1}$$

where

$$\overline{TDS} = \frac{1}{n}\sum_{j=1}^{n} P_j. \tag{2}$$

Then, in the uniformly scaling step, we have

$$\widehat{TDS} = [P_1 - \overline{TDS}, P_2 - \overline{TDS}, ..., P_n - \overline{TDS}]/\hat{\sigma}, \tag{3}$$

where

$$\hat{\sigma} = \sqrt{\frac{1}{n}\sum_{j=1}^{n}(P_j - \overline{TDS})^2}. \quad (4)$$

The vector $\widehat{TDS}$ is thus the transformed object for superimposition, namely the standardized RSS fingerprint. Similarly, the transformed objects of all the RSS vectors collected by the reference device are derived and stored in the database. Suppose that one of the standardized RSS vector stored in the database, namely $\widehat{RDS}$, is chosen for matching with the RSS vector $\widehat{TDS}$ from the TD. To evaluate the similarity between the two original curves in terms of their shapes, the Procrustes distance between the two vectors $\widehat{TDS}$ and $\widehat{RDS}$, termed signal tendency index (STI), is computed as follows

$$s = \|\widehat{TDS} - \widehat{RDS}\| \quad (5)$$

where $\|\cdot\|$ denotes the Euclidean norm.

After elementary mathematical operations (see Appendix A), we can obtain

$$s = \sqrt{2n(1-\rho)}, \quad (6)$$

where ρ denotes the sample Pearson product-moment correlation coefficient (PPMCC) [40] between the vectors TDS and RDS. Although (6) establishes an equivalence relation between the STI and sample PPMCC, it does not imply that the proposed STI method can be replaced by the sample PPMCC. To be specific, due to the ability of standardizing RSS fingerprints from heterogeneous and anonymous devices in an online fashion, the STI method can be applied to preprocess RSS fingerprints, so as to alleviate the effect of device heterogeneity on any RSS fingerprints based treatment that follows, whereas the sample PPMCC cannot be used in this way. For example, the STI method can be integrated with existing WiFi fingerprinting localization schemes, such as KNN based schemes, machine learning based schemes, and so on, to improve their robustness to heterogeneous devices; moreover, in any practical crowdsourcing based IPS (e.g. [19]–[23]), RSS fingerprints, which are normally collected at different times and from heterogeneous devices, can be firstly standardized by the STI method and then used for building the fingerprint database, which is helpful in mitigating the negative impact of device heterogeneity.

D. Theoretical Analysis

In the first place, we investigate why the STI method is robust to heterogeneous MDs from a theoretical perspective.

Without loss of generality, let the APs be transmitters and MDs be receivers. Suppose $P(d_j)$ denotes the RSS by a MD at an arbitrary distance d_j from the transmitter of the j-th AP. According to the LDPL model [41], we have

$$P(d_j)(\text{dBm}) = 10\log\left(\frac{\tau_j^2 G_j G_{MD} T_j}{16\pi^2}\right) - 10\alpha\log d_j + Z_j \quad (7)$$

where τ_j is the wavelength of the propagating signal in meter, G_j and G_{MD} are the transmitter and receiver antenna gains at the AP and MD, respectively, T_j is the signal transmission power, α is the path loss exponent, and Z_j is a random variable representing the shadowing effect in dBm which is assumed to be normally distributed with mean zero and variance σ_j^2. It is acknowledged that (7) holds only if d_j is beyond a closed-in reference distance. Accordingly, the mean RSS value can be expressed as follows:

$$\overline{P}(d_j)(\text{dBm}) = 10\log\left(\frac{\tau_j^2 G_j G_{MD} T_j}{16\pi^2}\right) - 10\alpha\log d_j \quad (8)$$

Since the values of parameters G_j, T_j and G_{MD} depend on the hardware of the AP and MD, if the same pair of AP and MD is considered, the relationship between the mean RSS value and the distance from the AP to the MD is one-to-one. But, if APs or MDs with different hardware are adopted, the corresponding relationship becomes many-to-one; that is to say, given one mean RSS value, there are multiple possible distances. Hence, with the WiFi fingerprinting technique, there exist certain discrepancies between a location and its fingerprint (i.e. the corresponding RSS values) if heterogeneous APs or MDs are used, which will degrade the IPS performance. This explains why device heterogeneity degrades the performance of the fingerprinting-based IPS.

Signal strength difference (SSD) is a location signature which leverages the differences of signals perceived at APs from a MD [10]. With the SSD method, if the first AP is used as reference AP, then the SSD associated with the j-th AP is produced as new fingerprints as follows

$$\begin{aligned} & P(d_j)(\text{dBm}) - P(d_1)(\text{dBm}) \\ = \;& 10\log\tfrac{\tau_j^2 G_j T_j}{\tau_1^2 G_1 T_1} - 10\alpha\log\tfrac{d_j}{d_1} + Z_j - Z_1 \end{aligned} \quad (9)$$

with $j = 2, \cdots, n$. As suggested in [10], since the parameter G_{MD} depending on the MD hardware does not exist in (9), the SSD is entirely free from the influence of the device heterogeneity caused by using different MDs. But, it is noticeable that the SSD variance is $\sigma_j^2 + \sigma_1^2$.

Using the STI method, the average RSS from all the APs, denoted by $\overline{TDS}$, can be formulated as follows

$$\begin{aligned} \overline{TDS}(\text{dBm}) \;=\; & \frac{10}{n}\sum_{p=1}^{n}\log(\tau_p^2 G_p T_p) + 10\log\frac{G_{MD}}{16\pi^2} \\ & - \frac{10\alpha}{n}\sum_{p=1}^{n}\log d_p + \frac{1}{n}\sum_{p=1}^{n} Z_p \end{aligned} \quad (10)$$

and the translating RSS associated with the j-th AP is

$$\begin{aligned} & P(d_j)(\text{dBm}) - \overline{TDS}(\text{dBm}) \\ = \;& 10\log(\tau_j^2 G_j T_j) - \frac{10}{n}\sum_{p=1}^{n}\log(\tau_p^2 G_p T_p) - 10\alpha\log d_j \\ & + \frac{10\alpha}{n}\sum_{p=1}^{n}\log d_p + Z_j - \frac{1}{n}\sum_{p=1}^{n} Z_p. \end{aligned} \quad (11)$$

It follows from (11) that the translating RSS in the STI method is uncorrelated with G_{MD} (i.e., the parameter depending on the MD hardware). In addition, according to (4) the scaling parameter s is uncorrelated with G_{MD} as well. Hence, it can be concluded that location fingerprints standardized by the STI method is immune to the device heterogeneity induced by MDs like the SSD method.

Furthermore, the variance of the translating RSS is equal to $\sigma_j^2 - 2\sigma_j/n + \sum_p \sigma_p^2/n^2$, which is generally small in comparison with the SSD method; e.g., if $\sigma_1 = \cdots = \sigma_n$ and $n \gg 1$, the variance in the STI method is much smaller than that in the SSD method. Since a small variance indicates a narrow range of fingerprints (e.g., translating RSS and SSD) associated with each physical location, it is accordingly easy to discriminate these locations through fingerprints. Therefore, it reveals that STI is superior to SSD, which is further verified by the experimental study in Section V.

Next, we analyze how the STI method improves the robustness to indoor environmental changes under certain conditions.

As pointed out in [41], in some environments, such as buildings, stadiums and other indoor environments, the path loss exponent (PLE) can take values in the range of 4 to 6. In a given indoor environment, if the number and distribution of objects, such as people, furniture, and so on, change over time, one constant PLE cannot accurately characterize the path attenuation at all times; that is to say, the fingerprint collected at one location during the site survey procedure will most likely deviate from its counterparts in the online phase due to indoor environmental changes, which inevitably impairs the robustness of the fingerprinting-based IPS.

On these grounds, define $\alpha + \Delta\alpha$ to be the real PLE in the online phase, where $\Delta\alpha$ reflects indoor environmental changes. Provided that the n APs are homogeneous or have similar hardware parameters (i.e. $G_1, \cdots, G_n$ and $T_1, \cdots, T_n$), (11) can be simplified as

$$P(d_j)(\text{dBm}) - \overline{TDS}(\text{dBm}) = Z_j - \frac{1}{n}\sum_{p=1}^{n} Z_p + (\alpha + \Delta\alpha)\left(-10\log d_j + \frac{10}{n}\sum_{p=1}^{n}\log d_p\right). \quad (12)$$

Equation (12) indicates that, given $G_1 = \cdots = G_n$ and $T_1 = \cdots = T_n$, the translating RSS $P(d_j)(\text{dBm}) - \overline{TDS}(\text{dBm})$ is just scaled by $\alpha + \Delta\alpha$ if ignoring the noise terms, and as a result, the shape of the fingerprint at this location is scaled in the same way as well. Considering the fact that the PA method is able to compare the shapes of objects under different scales, the scaling issue caused by the indoor environmental changes is thus mitigated when using the standardized fingerprint. However, when using the original fingerprinting technique and SSD, the scaling issue cannot be addressed, and the IPS performance will be degraded.

To sum up, the theoretical analysis reveals that the translating and scaling operations adopted in the STI method are able to alleviate the effect of device heterogeneity and indoor environmental changes. Moreover, it is also convenient to deduce similar conclusions as above if we let the MD be the transmitter and APs be receivers.

IV. Proposed STI-WELM Algorithm

In this section, we first introduce preliminaries on WELM, and then describe the structure of the proposed algorithm combining STI and WELM.

A. Preliminaries on WELM for Indoor Localization

Data in real applications such as RSS from different APs usually have imbalanced class distribution, which means some of the data are important than others in the database. WELM is proposed in [28] to tackle the regression or classification tasks with imbalanced class distribution. It inherits the advantages from original ELM, which is simple in theory that the hidden nodes are randomly generated and the output weight is analytically determined. It has therefore been adopted for easy and fast implementation [26], [27]. Furthermore, it is able to deal with data of imbalanced distributions by incorporating the information of imbalance dataset [28].

WELM is a machine learning algorithm based on a generalized Single-hidden Layer Feedforward neural Network (SLFN) architecture. As a machine learning algorithm, it requires a training process to establish the trained WELM model for online use. For the scenario of IPS, assume there are M WiFi RSS fingerprints in total collected at the RPs. These WiFi RSS fingerprints and their physical coordinates are adopted as training inputs and training targets respectively to build up the WELM model. As demonstrated in Table. I, each training sample can be represented as $(\mathbf{x}_i, \mathbf{t}_i) \in \mathbf{R}^M \times \mathbf{R}^2$, where the training input $\mathbf{x}_i = [RSS_i^1, RSS_i^2, \ldots, RSS_i^n]$ is a vector of RSS received from n APs in the environment, and training target $\mathbf{t}_i = (t_i^1, t_i^2)$ is the 2-D physical coordinates of the RP.

Assume that a SLFN with L hidden nodes can approximate these M samples with zero error, then there exist β_i, $\mathbf{a}_i$ and b_i such that

$$\mathbf{t}_i = \sum_{u=1}^{L} \beta_u G(\mathbf{a}_u, b_u, \mathbf{x}_i), i = 1, 2, \ldots, M, \quad (13)$$

where $\mathbf{a}_u$ and b_u are the learning parameters of the hidden nodes, β_u is the output weight, and $G(\mathbf{a}_u, b_u, \mathbf{x}_i)$ is the activation function which gives the output of the uth hidden node with respect to the input $\mathbf{x}_i$.

Given M arbitrary distinct training samples $(\mathbf{x}_i, \mathbf{t}_i), i = 1, 2, \ldots, M$, by substituting $\mathbf{x}$ with $\mathbf{x}_i$ in Eq. 13 we obtain

$$\boldsymbol{H}\boldsymbol{\beta} = \mathbf{T} \quad (14)$$

where

$$\mathbf{H} = \begin{bmatrix} G(\mathbf{a}_1, b_1, \mathbf{x}_1) & \ldots & G(\mathbf{a}_L, b_L, \mathbf{x}_1) \\ \vdots & \ldots & \vdots \\ G(\mathbf{a}_1, b_1, \mathbf{x}_M) & \ldots & G(\mathbf{a}_L, b_L, \mathbf{x}_M) \end{bmatrix}_{M\times L} = \begin{bmatrix} \mathbf{h}(\mathbf{x}_1) \\ \mathbf{h}(\mathbf{x}_2) \\ \vdots \\ \mathbf{h}(\mathbf{x}_M) \end{bmatrix}_{M\times L}, \quad (15)$$

$$\boldsymbol{\beta} = \begin{bmatrix} \beta_1^T \\ \vdots \\ \beta_L^T \end{bmatrix}_{L\times 2} \text{ and } \mathbf{T} = \begin{bmatrix} \mathbf{t}_1^T \\ \vdots \\ \mathbf{t}_M^T \end{bmatrix}_{M\times 2}. \quad (16)$$

In the above, $\mathbf{H}$ is the hidden layer output matrix, $\boldsymbol{\beta}$ is the output weight matrix and $\mathbf{T}$ is the training target matrix of WELM; the uth column of $\mathbf{H}$ is the uth hidden node's output vector with respect to inputs $x_1, x_2, \ldots, x_M$, and the

TABLE I
TRAINING INPUT $\mathbf{x}$ AND TRAINING TARGET $\mathbf{t}$ FOR WIFI RSS FINGERPRINT DATABASE

Training input $\mathbf{x}$, $RSS(dBm)$								Training target $\mathbf{t}$, (m)
AP_1	AP_2	AP_3	AP_4	AP_5	AP_6	AP_7	AP_8	2-D physical coordinates
-32	-95	-63	-53	-79	-47	-69	-49	(2.55 10.68)
-90	-84	-73	-65	-58	-43	-59	-37	(12.16 23.73)
⋮				⋱				
RSS_i^1	RSS_i^2	RSS_i^3	RSS_i^4	RSS_i^5	RSS_i^6	RSS_i^7	RSS_i^8	(t_i^1, t_i^2)
⋮				⋱				
RSS_M^1	RSS_M^2	RSS_M^3	RSS_M^4	RSS_M^5	RSS_M^6	RSS_M^7	RSS_M^8	(t_M^1, t_M^2)

ith row of $\mathbf{H}$ is the output vector of the hidden layer with respect to the input vector of x_i. Unlike the traditional training algorithms for neural networks which adjust the input weights and hidden layer biases, [26] proved that the parameters of SLFN can be randomly assigned if the activation function is infinitely differentiable. Therefore, the hidden layer output matrix H remains unchanged once these parameters are randomly initialized. After that, an $M \times M$ diagonal matrix $\mathbf{W}$ is defined which is associated with every training sample $\mathbf{x}_i$.

Regarding the IPS, we apply WELM to solve the localization problem by regression, namely minimizing the weighted cumulative localization error with respect to each training sample $(\mathbf{x}_i, \mathbf{t}_i)$, which can be mathematically written as

$$\begin{aligned} \min_{\boldsymbol{\xi}, \boldsymbol{\beta} \in \mathbf{R}^{L \times 2}} \quad & L_P = \frac{1}{2}\|\boldsymbol{\beta}\|^2 + W\frac{C}{2}\sum_{i=1}^{M}\xi_i \\ s.t. \quad & \mathbf{h}(\mathbf{x}_i)\boldsymbol{\beta} = t_i^T - \xi_i^T \qquad i = 1, 2, \ldots, M \end{aligned} \tag{17}$$

where ξ_i is the training error of $\mathbf{x}_i$, which is caused by the difference of the output $\mathbf{h}(\mathbf{x}_i)\boldsymbol{\beta}$ and desired output t_i, and C is a hyper-parameter for better generalization performance [42]. The solution of the output weight vector $\boldsymbol{\beta}$ is analytically determined using the Moore-Penrose generalized inverse $\hat{\mathbf{H}}$. Dependent on the size of training samples, there are two versions of solutions of $\boldsymbol{\beta}$:

$$\boldsymbol{\beta} = \begin{cases} \mathbf{H^T}(\frac{\mathbf{I}}{C} + \mathbf{WHH^T})^{-1}\mathbf{WT}, & M < L \\ (\frac{\mathbf{I}}{C} + \mathbf{H^T WH})^{-1}\mathbf{H^T WT}, & M > L \end{cases} \tag{18}$$

It can be seen from the above two formulas that a positive definite matrix $\mathbf{I}/C$ is added to the diagonal of $\mathbf{WHH^T}$ or $\mathbf{H^T WH}$. Since the weight matrix $\mathbf{W} = diag(W_{ii}), i = 1, ..., M$ is significant in WELM, two weighting schemes are proposed in [28]. One weighting scheme assigns a unified W_{ii} to each sample, the other adopts the value of golden standard that represents the perfection in nature. However, both of these weighting schemes are static and have not considered the importance of each training sample. We shall propose a new weight scheme in Section IV.B. which assigns different weight to each sample according to its significance.

In summary, the training process of WELM is conducted in the following three main steps:

Step 1: Randomly assign the input parameters: input weights $\mathbf{a}_u$ and biases b_u, $u = 1, \ldots, L$.

Step 2: Calculate the hidden layer output matrix $\mathbf{H}$ and the weight matrix $\mathbf{W}$.

Step 3: Calculate the output weight $\boldsymbol{\beta}$.

B. STI-WELM

The proposed STI-WELM algorithm inherits the merits of both STI and WELM, and consists of two main phases: online construction phase and online localization phase.

1) Online Construction Phase: The skeleton of the online construction procedure is depicted in Algorithm 1.

Algorithm 1 STIWELM

1. Construct TDS_{new} based on STI measurements
2. Build up the WiFi RSS fingerprint database for STI-WELM training
3. Construct the weight matrix W of STI-WELM
4. Establish the trained STI-WELM model for online localization

First of all, we calculate the STI value s_i between TDS and each RDS_i. Since a smaller s_i indicates that RDS_i is more similar with TDS, we further define a weight value w_i for each RDS_i, which is calculated as follows:

$$w_i = \frac{\frac{1}{s_i}}{\sum_{i=1}^{m}\frac{1}{s_i}} \tag{19}$$

Then, the m RPs are sorted according to their w_i in a descending order. For the next step, we reconstruct the TDS according to the RSS values RDS_i collected by the RD at the Q RPs, with their corresponding w weight values being larger than a threshold w_{th} (setting $w_t = 0.01$ in general), to alleviate the negative effect of device heterogeneity between TD and RD. For those RPs whose corresponding w weight values are smaller than w_{th}, their RSS values are discarded since they are not critical for localization anymore.

The TDS_{new} is calculated based on the following formula,

$$TDS_{new} = \frac{1}{\sum_{q=1}^{Q}\frac{1}{s_q}}\sum_{q=1}^{Q} RDS_q \cdot \frac{1}{s_q} \tag{20}$$

It can be seen from the above equation that TDS_{new} is constructed from $RDS_q, q = 1, ..., Q$ at the Q RPs, which means that it is more relevant to the RSS vectors in the database than the raw TDS.

The next step is to build up a WiFi RSS fingerprint database for STI-WELM training process. Unlike conventional fingerprinting-based IPS which requires to put the RSS fingerprints collected at all m RPs into a database for training, STI-WELM only requires to leverage the RSS fingerprints from the Q RPs whose corresponding w weight values are

larger than w_{th} to build up the database. It largely reduces the computational burden for the training process. Suppose f RSS fingerprints are collected at each RP. Therefore, the training set of STI-WELM becomes a $fQ \times n$ matrix, where the order of the f RSS fingerprints collected at each RP is based on its w weight values from the largest to the smallest.

After that, construct the weight matrix W for the STI-WELM training process. Note that the two weighting schemes proposed in [28] are generated regardless of the special property of training samples. On the contrary, in our scheme, the weight vector for each RSS fingerprint is designed elaborately based on its corresponding STI value s_q, namely

$$W = \frac{1}{\sum_{q=1}^{Q} \frac{1}{s_q}} \text{diag}(\frac{1}{s_1}, \ldots, \frac{1}{s_Q}) \otimes I_f, \tag{21}$$

where I_f is the identity matrix of order f and $\otimes$ denotes the Kronecker product. Then, these fQ RSS fingerprints and their corresponding physical locations are adopted as the training inputs $\mathbf{x}$ and the training targets $\mathbf{t}$ respectively for STI-WELM offline training. Similarly to WELM, the STI-WELM model will be trained as mentioned in Section IV. A. The detailed steps are illustrated below:

Step 1: Randomly assign the input parameters: input weights $\mathbf{a}_u$ and biases b_u, $u = 1, \ldots, L$.

Step 2: Calculate the hidden layer output matrix $\mathbf{H}$ and the weight matrix $\mathbf{W}$.

Step 3: Calculate the output weight $\boldsymbol{\beta}$.

Additionally, the activation function G and the number of hidden nodes L will be selected carefully in order to guarantee the performance of STI-WELM. A guideline for these parameter selections is presented in Section V. B. 3.). The STI-WELM model can be obtained quickly due to the fast training speed of WELM.

2) Online Localization Phase: When a user sends a location query with the real-time TDS measurement, by feeding the TDS to the trained STI-WELM model, the output of the model is the estimated location of the user.

V. Experimental Study

Extensive experiments were conducted to evaluate the performance of the proposed STI-WELM localization scheme. We first describe the setup of our testbed, and then detail the experimental results and performance evaluation.

A. System Setup and Data Collection Procedure

The testbed for our experiments was installed at the Internet of Things Laboratory of the School of Electrical and Electronic Engineering, Nanyang Technological University. The total area of the lab is around $580m^2$ $(35.1m \times 16.6m)$. 36 graduate students and 15 undergraduate students work and study regularly in this lab. Fig. 2 illustrates the layout of the lab, in which 8 Linksys WRT54GS WiFi routers were installed as APs for our experiments. All the APs were fixed on 1.9-meter-high tripods to keep them on the same height level.

To examine the influence of device heterogeneity, we employed 5 different mobile devices in our experiments, including iPhone 5S (Phone), iPad Air (Tablet), Nokia E71 (Phone), Samsung Galaxy Tab (Tablet) and Fujitsu LifeBook T4220 (Laptop). Table II summarizes the detail information of these devices. A script program was developed and ran on all the APs in order to collect RSS fingerprints associated with each mobile device from multiple APs. By leveraging this program, the APs were able to scan the 802.11 packets transmitted between mobile devices and APs so as to retrieve the RSS information of each packet, and then send the RSS value and the MAC address of the corresponding mobile device to a master AP which is connected to a central server. The server will store the RSS fingerprints and further apply our proposed STI-WELM algorithm to estimate the location of each device.

TABLE II
Mobile devices used for data collection

Device	WiFi Module	OS
iPhone 5S	Broadcom BCM4334	iOS 8
iPad Air	Broadcom BCM43241	iOS 8
Nokia E71	Wi-Fi 802.11 b/g	Symbian 9.2
Samsung Tablet	TI OMAP4430	Android 4.2
Fujitsu Laptop	Intel Wireless WiFi Link 4965AGN	Windows 7

Specifically, we collected RSS fingerprints of the five mobile devices at 54 different points, including 40 offline calibration points and 14 online testing points, as shown in Fig. 2. For each mobile device, 500 RSS fingerprints were collected at each point. The grid spacing between two adjacent locations of the calibration points was chosen to be larger than 1.25m based on the analysis in [43]. At each point, the mobile device was put on a 1.65-meter-high plastic cart for collecting WiFi RSS fingerprints.

B. Comparison between RSS, SSD and STI as Location Fingerprints

First of all, we evaluate the performance of the location fingerprints coming from the RSS, SSD and STI. Take the RSS for example. We first include all the RSS fingerprints of five mobile devices at each point into a fingerprint set of size 2500, calculate the sample standard deviation associated with each AP, and evaluate the average standard deviation from the 8 APs to measure the stability of the location fingerprints at this point. Likewise, we can calculate the average standard deviations for the location fingerprints used in SSD and STI. Note that, to make a fair comparison, the location fingerprints in the STI method only involve the translating operation.

Fig. 3 demonstrates the distribution histograms of the average standard deviations at the given 54 points with respect to the RSS, SSD and STI. As can be seen, the average standard deviation of STI is basically within 6 dBm, while those of the RSS and SSD are large and much widely scattered, which means that STI results in more stable and reliable location fingerprints than the others.

C. Experimental Results and Evaluation

Two well-known localization algorithms, namely K Nearest Neighbor (KNN) [6] and extreme learning machine (ELM) [26], are chosen in order to further compare their performance when RSS, SSD and STI are applied as the location fingerprint.

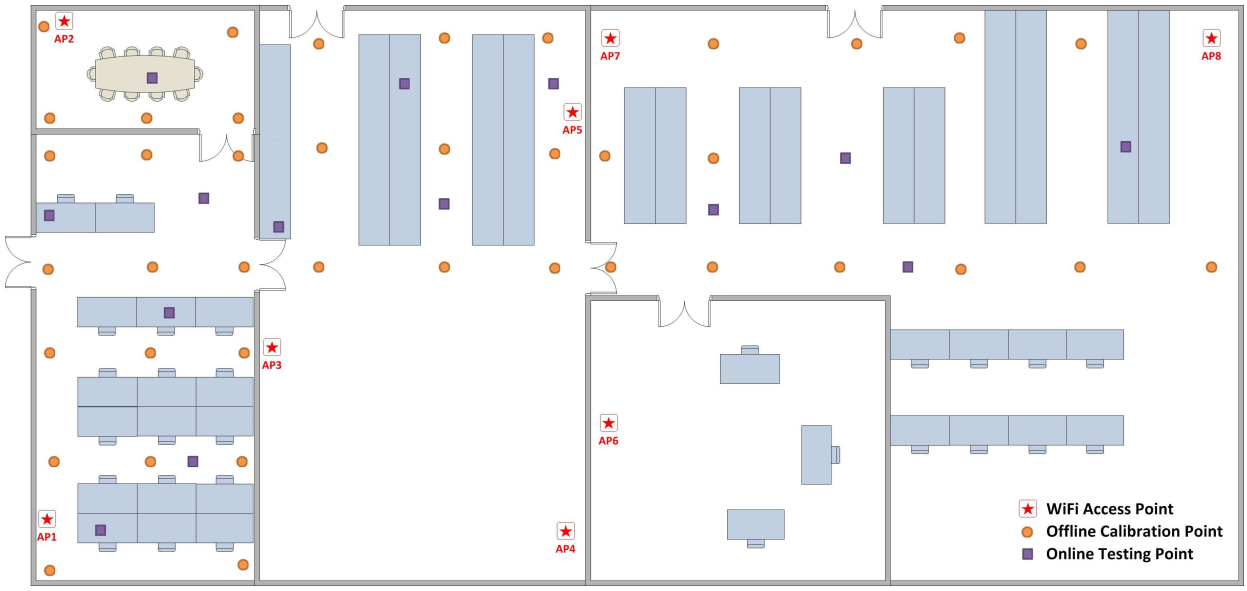

Fig. 2. Layout of the testbed

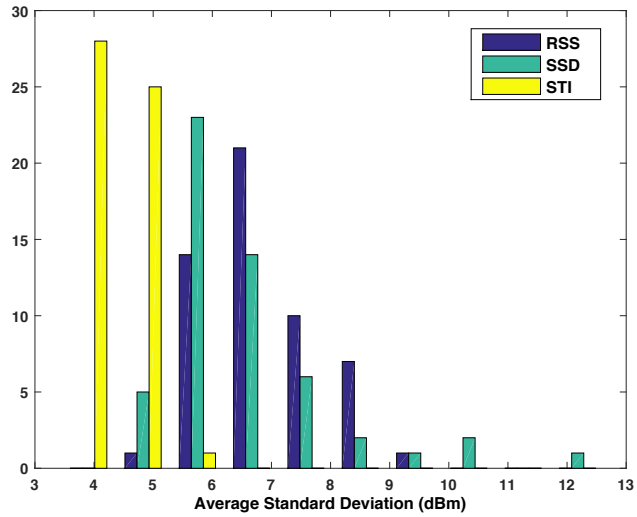

Fig. 3. Distribution Histogram of the Average Standard Deviations of Different Location Fingerprints

We include KNN into the comparison because of its wide usage as one of the classical localization algorithms. Furthermore, it has been shown in [18] that KNN-based approaches are superior to Bayesian Inference (BI) based approaches [14] when the reference device and the testing devices are different. Therefore, we include KNN instead of BI into our performance comparison and evaluation. For KNN, the value of K is determined empirically case-by-case according to the related WiFi RSS fingerprints database of the reference device. During the online phase, by matching the measured WiFi RSS fingerprints with the K closest WiFi RSS fingerprints in the database, the location of the target will be calculated. The algorithm is the same as in [6].

It has been shown in [36] that the performance of ELM in terms of the offline training time, the online testing time and the average localization accuracy are better than classical machine learning algorithms such as Back-propagation (BP) algorithm and support vector machine for regression (SVR) algorithm. Therefore we also choose ELM as the localization algorithm when RSS, SSD and STI are applied as the localization fingerprint respectively. The methodology of it is introduced in [36].

In practice, it is more likely for the users to carry different devices from the reference device. Therefore, we only analyze the situations that the testing device and reference device are distinct in our experiments.

By leveraging the 500×40 WiFi RSS fingerprints at the 40 offline calibration points of each device, the offline RSS, SSD and STI location fingerprint databases are established. The 500×14 WiFi RSS fingerprints at the online testing points of each device are utilized for the performance evaluation of each localization algorithm. The distance error is used to measure the localization accuracy of each approach. We define the location estimation error e to be the distance between the real location coordinates (x_0, y_0) and the system estimated location coordinates (x, y), i.e.:

$$e = \sqrt{(x - x_0)^2 + (y - y_0)^2} \tag{22}$$

Since we utilize 5 mobile devices in our experiments, there are 20 different combinations of reference device and testing device.

1) Comparison between STI-KNN without scaling and STI-KNN: In order to evaluate the influence of the uniform scaling step of STI on the localization accuracy, we compare the performance of STI-KNN with and without scaling step in the first place. The value of K is chosen to be 13 for this experiment.

The specific average localization errors given different combinations of reference devices and testing devices are

TABLE III
DETAILED AVERAGE LOCALIZATION ERRORS (IN METER) OF STI-KNN WITHOUT SCALING AND STI-KNN

Testing Dataset	STI-KNN without scaling	STI-KNN
Training Dataset: iPhone 5S		
iPad Air	3.107	**2.959**
Nokia E71	3.717	**3.716**
Samsung Tablet	3.836	**3.777**
Fujitsu Laptop	2.983	**2.927**
Average	3.411	**3.345**
iPhone 5S	2.424	**2.398**
Training Dataset: iPad Air		
iPhone 5S	3.445	**3.339**
Nokia E71	3.653	**3.639**
Samsung Tablet	3.706	**3.612**
Fujitsu Laptop	2.877	**2.875**
Average	3.420	**3.366**
iPad Air	2.849	**2.813**
Training Dataset: Nokia E71		
iPhone 5S	3.630	**3.552**
iPad Air	3.093	**3.029**
Samsung Tablet	3.850	**3.746**
Fujitsu Laptop	3.132	**3.126**
Average	3.426	**3.363**
Nokia E71	2.798	**2.736**
Training Dataset: Samsung Tablet		
iPhone 5S	3.555	**3.483**
iPad Air	3.050	**2.989**
Nokia E71	3.728	**3.673**
Fujitsu Laptop	3.079	**3.019**
Average	3.353	**3.291**
Samsung Tablet	2.761	**2.743**
Training Dataset: Fujitsu Laptop		
iPhone 5S	3.758	**3.385**
iPad Air	3.268	**2.950**
Nokia E71	3.844	**3.611**
Samsung Tablet	4.056	**3.653**
Average	3.731	**3.400**
Fujitsu Laptop	2.832	**2.734**

TABLE IV
DETAILED AVERAGE LOCALIZATION ERRORS (IN METER) UNDER VARIOUS SITUATIONS (KNN)

Testing Dataset	RSS-KNN	SSD-KNN	STI-KNN
Training Dataset: iPhone 5S			
Best K for KNN	*13*	*12*	*13*
iPad Air	4.738	3.778	**2.959**
Nokia E71	4.263	4.326	**3.716**
Samsung Tablet	4.447	4.723	**3.777**
Fujitsu Laptop	4.892	3.344	**2.927**
Average	4.585	4.043	**3.345**
Training Dataset: iPad Air			
Best K for KNN	*13*	*15*	*13*
iPhone 5S	4.154	4.388	**3.339**
Nokia E71	4.698	4.404	**3.639**
Samsung Tablet	4.651	4.549	**3.612**
Fujitsu Laptop	3.576	3.235	**2.875**
Average	4.270	4.144	**3.366**
Training Dataset: Nokia E71			
Best K for KNN	*14*	*13*	*13*
iPhone 5S	3.914	4.576	**3.552**
iPad Air	4.434	4.287	**3.029**
Samsung Tablet	4.001	4.909	**3.746**
Fujitsu Laptop	4.586	3.810	**3.126**
Average	4.234	4.395	**3.363**
Training Dataset: Samsung Tablet			
Best K for KNN	*15*	*12*	*13*
iPhone 5S	4.074	4.450	**3.483**
iPad Air	4.957	4.197	**2.989**
Nokia E71	4.152	4.545	**3.673**
Fujitsu Laptop	5.154	3.705	**3.019**
Average	4.584	4.224	**3.291**
Training Dataset: Fujitsu Laptop			
Best K for KNN	*13*	*11*	*13*
iPhone 5S	5.209	4.856	**3.385**
iPad Air	3.972	4.277	**2.950**
Nokia E71	5.986	4.946	**3.611**
Samsung Tablet	5.644	5.187	**3.653**
Average	5.203	4.816	**3.400**

demonstrated in Table III. As can be seen, STI-KNN can provide higher localization accuracy in every situation when the uniform scaling step is involved in the procedure. In general, the uniform scaling step enhances the precision of indoor positioning of STI-KNN by 3.09%. Therefore, we can conclude that, the uniform scaling step could facilitate STI to mitigate the effect of indoor environmental dynamics.

2) Comparison among RSS-KNN, SSD-KNN and STI-KNN: Two location fingerprints: RSS and SSD are leveraged and integrated with the KNN localization algorithm to compare with STI-KNN. Since the value of K is critical for the performance of KNN approaches when the reference device is altered, we analyze the performance of RSS-KNN, SSD-KNN and STI-KNN with all the possible values of K, and compare their best performance in each scenario (20 different combinations of reference device and testing device). Table IV demonstrates the specific average localization errors of each combination of reference device and testing device of these three approaches with their best performances given the optimal K value.

It is evident from Table IV that STI-KNN provides higher localization accuracy than RSS-KNN and SSD-KNN in every situation. Fig. 4 depicts the distance error distribution of the three approaches when each mobile device is leveraged as the reference device. Similar to the results shown in Table IV, STI-KNN has the best performance among the three approaches in terms of localization accuracy.

To summarize, as shown in Table V, STI-KNN can enhance the precision of indoor positioning by 26.71% over RSS-KNN and 22.47% over SSD-KNN respectively. Thus, when KNN is employed as the localization algorithm, the proposed STI method can largely alleviate the effect of device heterogeneity and provide robust and high indoor positioning service consistently even the testing devices are different from the reference device.

3) Comparison between RSS-ELM, SSD-ELM, STI-ELM and STI-WELM: As a fingerprinting-based IPS, the relevant ELM models for online localization are required to be built up during the online construction phase. For RSS-ELM, the RSS-ELM model is built up by adopting the 500×40 WiFi RSS fingerprints collected at the 40 offline calibration points. These WiFi RSS fingerprints and their physical locations are adopted as training inputs and training targets respectively to build up the model. For the construction of SSD-ELM model, the 500×40 WiFi RSS fingerprints collected at the offline calibration points are transferred into SSD format first. Then the model is built up in the similar process as RSS-ELM. During the online testing phase, the raw RSS vectors measured by TD are reconfigured into the SSD format and put into the

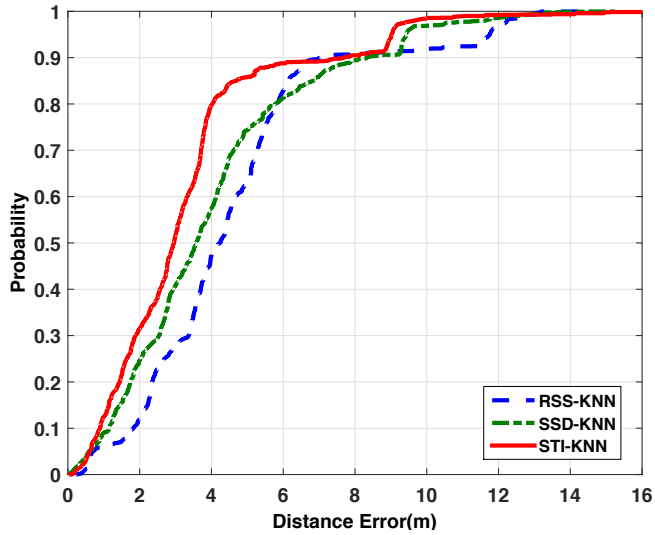

(a) Training dataset: iPhone 5S

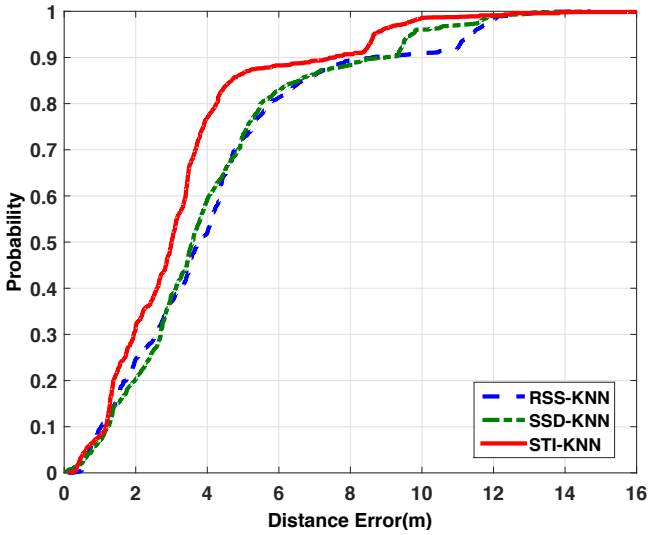

(b) Training dataset: iPad Air

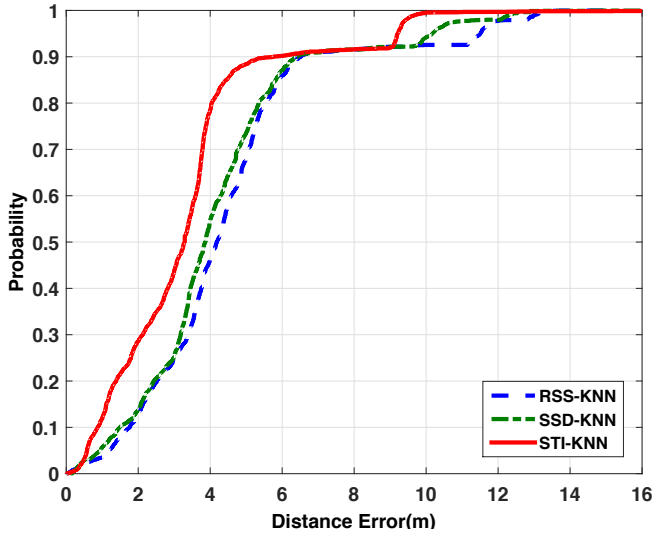

(c) Training dataset: Nokia E71

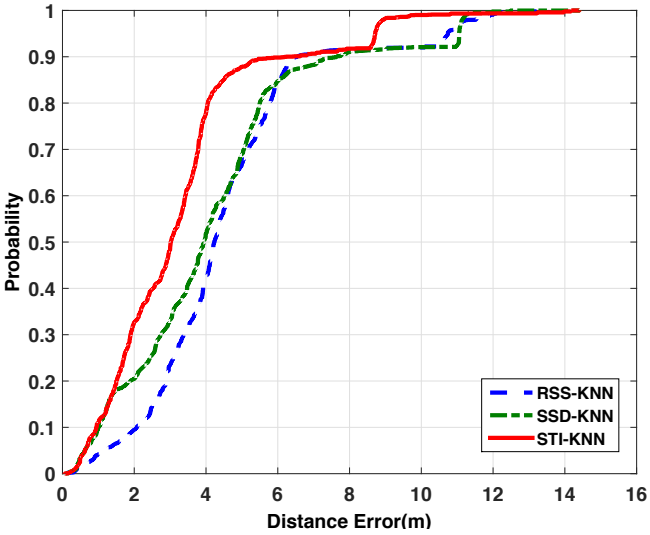

(d) Training dataset: Samsung Tablet

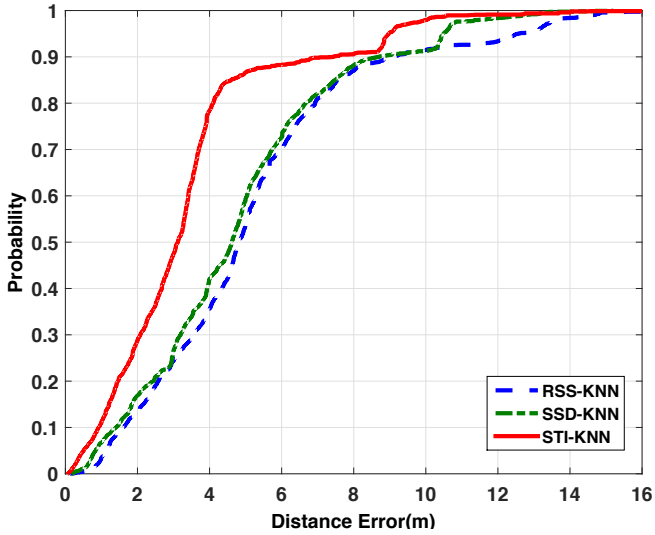

(e) Training dataset: Fujitsu Laptop

Fig. 4. Comparison of Distance Error Distributions for different methods

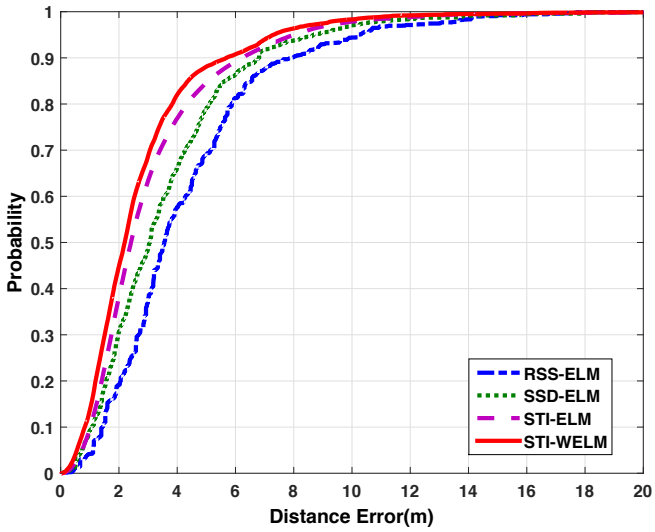

(a) Training dataset: iPhone 5S

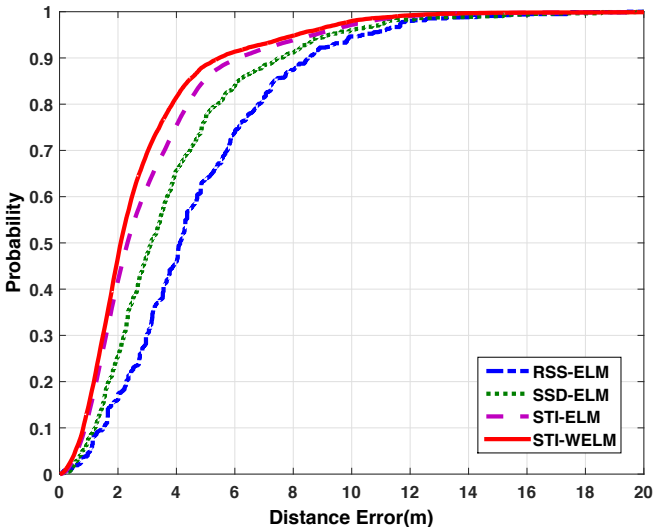

(b) Training dataset: iPad Air

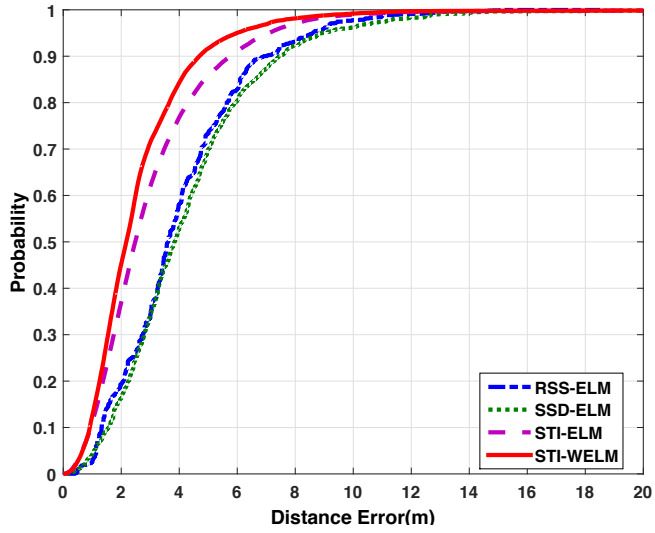

(c) Training dataset: Nokia E71

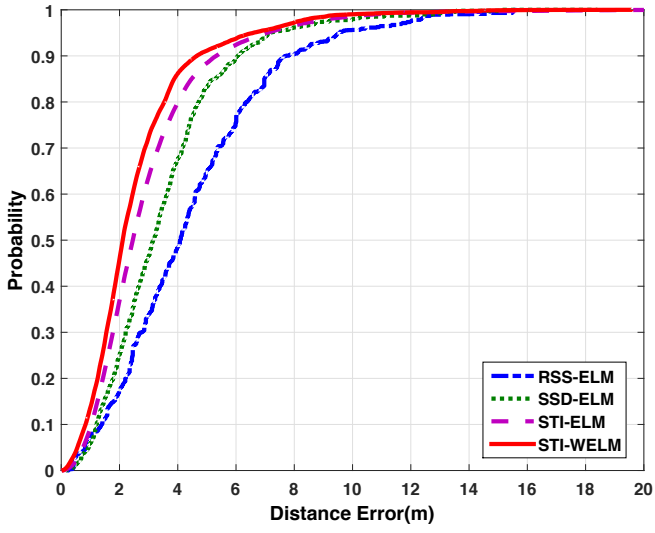

(d) Training dataset: Samsung Tablet

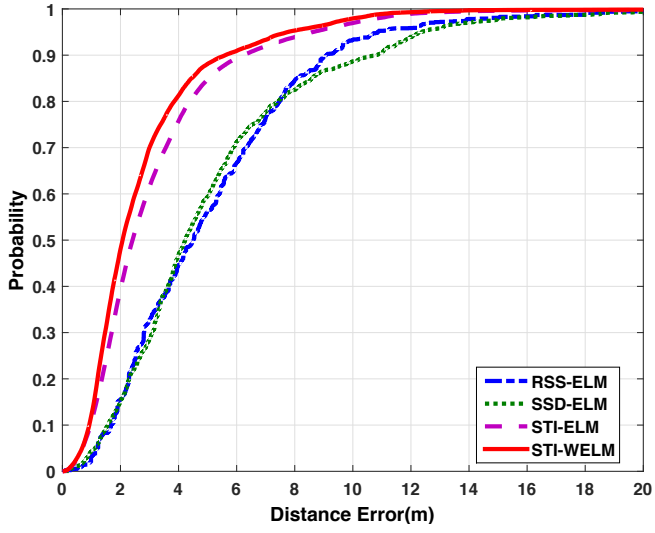

(e) Training dataset: Fujitsu Laptop

Fig. 5. Comparison of Distance Error Distributions for different methods

TABLE V
SUMMARY OF AVERAGE LOCALIZATION ERRORS (IN METER) (KNN)

Training Dataset	RSS-KNN	SSD-KNN	STI-KNN	STI-KNN VS RSS-KNN (%)	STI-KNN VS SSD-KNN (%)
iPhone 5S	4.585	4.043	3.345	27.5	17.27
iPad Air	4.270	4.144	3.366	21.16	18.77
Nokia E71	4.234	4.395	3.363	20.56	23.48
Samsung Tablet	4.584	4.224	3.291	28.21	22.09
Fujitsu Laptop	5.203	4.816	3.400	34.65	29.42
Average	**4.575**	**4.325**	**3.353**	**26.71**	**22.47**

TABLE VII
SUMMARY OF AVERAGE LOCALIZATION ERRORS (IN METER) (ELM)

Training Dataset	RSS-ELM	SSD-ELM	STI-ELM	STI-WELM	STI-WELM VS RSS-ELM (%)	STI-WELM VS SSD-ELM (%)	STI-WELM VS STI-ELM (%)
iPhone 5S	4.301	3.611	3.121	2.793	35.06	22.65	10.51
iPad Air	4.690	3.827	3.088	2.791	40.48	27.07	9.61
Nokia E71	4.020	4.288	3.005	2.599	35.34	39.38	13.49
Samsung Tablet	4.463	3.498	2.946	2.591	41.95	25.93	12.07
Fujitsu Laptop	5.113	5.201	3.172	2.803	45.17	46.10	11.62
Average	**4.517**	**4.085**	**3.066**	**2.715**	**39.89**	**33.54**	**11.45**

TABLE VI
DETAILED AVERAGE LOCALIZATION ERRORS (IN METER) UNDER VARIOUS SITUATIONS (ELM)

Testing Dataset	RSS-ELM	SSD-ELM	STI-ELM	STI-WELM
Training Dataset: iPhone 5S				
iPad Air	4.368	2.927	2.494	**2.084**
Nokia E71	4.240	4.529	3.825	**3.543**
Samsung Tablet	5.221	4.372	3.689	**3.474**
Fujitsu Laptop	3.374	2.616	2.476	**2.070**
Average	4.301	3.611	3.121	**2.793**
iPhone 5S	4.260	3.367	2.507	**2.237**
Training Dataset: iPad Air				
iPhone 5S	4.378	3.909	3.039	**2.732**
Nokia E71	5.567	4.808	3.689	**3.344**
Samsung Tablet	5.146	3.874	3.331	**3.136**
Fujitsu Laptop	3.669	2.718	2.295	**1.953**
Average	4.690	3.827	3.088	**2.791**
iPad Air	3.684	3.552	2.176	**1.842**
Training Dataset: Nokia E71				
iPhone 5S	4.181	4.328	3.410	**3.090**
iPad Air	4.148	3.849	2.497	**1.988**
Samsung Tablet	4.336	5.180	3.569	**3.293**
Fujitsu Laptop	3.414	3.793	2.542	**2.025**
Average	4.020	4.288	3.005	**2.599**
Nokia E71	3.965	4.113	2.761	**2.334**
Training Dataset: Samsung Tablet				
iPhone 5S	4.140	3.775	3.207	**2.933**
iPad Air	4.718	3.097	2.392	**2.001**
Nokia E71	5.390	4.158	3.651	**3.267**
Fujitsu Laptop	3.603	2.960	2.534	**2.160**
Average	4.463	3.498	2.946	**2.591**
Samsung Tablet	4.126	2.238	2.592	**2.439**
Training Dataset: Fujitsu Laptop				
iPhone 5S	6.770	5.473	3.128	**2.687**
iPad Air	3.365	4.090	2.459	**2.087**
Nokia E71	5.811	5.931	3.726	**3.362**
Samsung Tablet	4.504	5.309	3.375	**3.076**
Average	5.113	5.201	3.172	**2.803**
Fujitsu Laptop	3.816	4.449	2.242	**2.081**

trained SSD-ELM model, then the estimated location of the TD will be calculated.

For STI-ELM and STI-WELM, as mentioned in Section IV. B, only WiFi RSS fingerprints collected by the RD at the Q RPs are adopted for building up the STI-ELM model and STI-WELM model. Therefore, the training process of these two approaches are much faster than RSS-ELM and SSD-ELM, which require to train the WiFi RSS fingerprints at all the 40 offline calibration points. In our experiments, we select Q to be 13 because the w weight value of these Q RPs are larger than $w_{th} = 0.01$. Therefore, the size of training database is largely reduced from 500×40 to 500×13. The performance of three activation functions: radial basis function (RBF) $G(a, b, x) = e^{-b||x-a||^2}$, sine function $G(a, b, x) = sin(ax + b)$ and hard-limit transfer (hardlim) function $G(a, b, x) = hardlim(ax + b)$ are analyzed by leveraging the offline WiFi RSS fingerprints database. The hardlim function is chosen since it provides the best performance among the three activation functions. Another critical parameter for the performance of the ELM based approaches is the number of hidden nodes L. The five-fold cross-validation method is employed with a range from 1 to 100 and a step size of 2 in order to determine the optimal L. After comprehensive evaluations on both localization accuracy and repeatability, L is selected to be 23 for both STI-ELM and STI-WELM. Based on our experimental results, these two approaches only spend 0.056s on average to calculate the output weights β for the $(500 \times 13 = 6500)$ WiFi RSS fingerprints during the training process.

A guideline for selecting the type of activation function and the number of hidden nodes in the STI-WELM hidden layer, both of which are the critical parameters for the performance of the STI-WELM approach, is listed as follows: the suggested default activation function for the STI-WELM approach is the hardlim function, whose performance is better than others in general; as for the optimal number of hidden nodes, the five-fold cross-validation method is employed with a range from

TABLE VIII
SUMMARY OF AVERAGE LOCALIZATION ERRORS (IN METER) UNDER THE INFLUENCE OF THE NUMBER OF APS

Number of APs	RSS-ELM	STI-ELM	STI-WELM
3	5.615	4.711	**4.636**
4	5.307	4.337	**4.157**
5	5.254	4.289	**3.562**
6	5.149	4.107	**3.092**
7	4.883	3.518	**2.756**
8 (All)	4.517	3.066	**2.715**

0 to 100 and a step size of 2 based on the empirical tuning.

The weight matrix W of STI-WELM is calculated according to our proposed weighting scheme as introduced in Section IV.B. Similar to the KNN experiments, there are 20 different combinations of reference device and testing device because 5 mobile devices are employed in the ELM experiments.

The specific average localization errors of each combination of reference device and testing device when RSS-ELM, SSD-ELM, STI-ELM and STI-WELM are adopted are demonstrated in Table VI respectively. It can be seen from Table VI that its localization performance trumps other three approaches significantly in every combination. It is also noteworthy that the performance of STI-ELM is better than RSS-ELM and SSD-ELM. The mean localization accuracies of RSS-ELM and SSD-ELM are almost the same. The distance error distribution of the four approaches when each mobile device is leveraged as the reference device are present in Fig. 5. As observed in Fig. 5, STI-WELM provides the most accurate indoor positioning service among the four approaches, which is consistent with the results demonstrated in Table VI.

In summary, STI-WELM enhances the precision of indoor positioning by 39.89% over RSS-ELM, 33.54% over SSD-ELM and 11.45% over STI-ELM respectively. Table VII summarizes the performance of each approach. Therefore, the proposed STI-WELM can provide more robust, fast and accurate indoor positioning service than other approaches consistently, and alleviate the effect of heterogeneous issue among different devices remarkably. Furthermore, another noteworthy point is that the performance of both ELM and WELM is better than KNN provided that the same type of the location fingerprint is adopted. This claim is supported by Fig. 4 and Fig. 5, in which the curves produced by ELM and WELM based algorithms are smoother than KNN based ones, i.e., the ELM and WELM based approaches are more robust to outliers.

In addition, iPad Air and Fujitsu Laptop obtain the best overall localization accuracy among all the devices considered, which is contributable to their relative high transmission powers; see the resulting RSS values in relation to different devices in Fig. 1.

4) Performance evaluation of STI-WELM under the influence of the number of APs : The aforementioned section has demonstrated the superiority of STI-WELM to alleviate the effect of heterogeneous devices for indoor localization when all the APs in the testbed were leveraged. In this subsection, we further analyze the performance of STI-WELM under the influence of the number of APs.

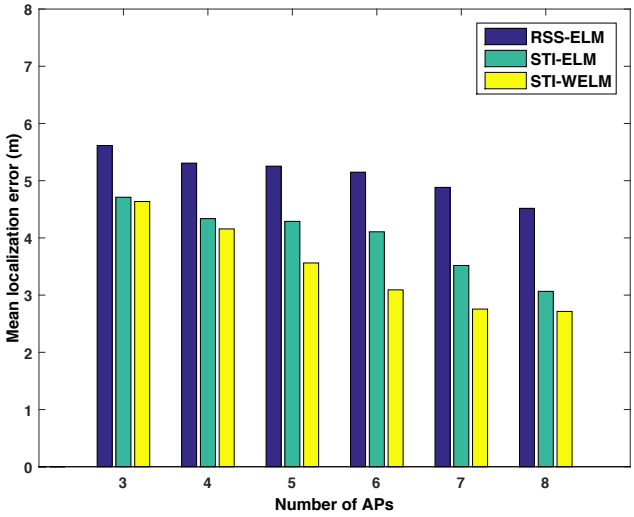

Fig. 6. Comparison of mean localization error between different approaches under the influence of the number of APs.

We compare the performance of STI-WELM with RSS-ELM and STI-ELM when the number of APs is altered. The training processes of these approaches are the same as is introduced in Section V.B.3). We consider all the 20 different combinations of reference device and testing device for this experiment as well, since 5 different mobile devices are utilized in total. The overall performance in terms of mean localization errors between these approaches under different numbers of APs is demonstrated in Fig. 6 and Table VIII.

As shown in Table VIII, the mean localization errors of all the three approaches decrease as the number of APs in-use increases. It can be easily observed that STI-WELM outperforms RSS-ELM and STI-ELM in every situation. The performance of RSS-ELM is the worst in all situations since it leverages the raw RSS data of testing device and the large localization error is caused by device heterogeneity. On the contrary, after the operations of translation and uniformly scaling in STI, the newly constructed TDS_{new} is more relevant to the RSS fingerprints stored in the reference device database. This is the main reason why both STI-ELM and STI-WELM are superior to RSS-ELM. By considering the relative importance of each RSS sample according to its corresponding STI value in the reference device database and leveraging our proposed weighting scheme, the localization accuracy of STI-WELM is higher than that of STI-ELM in general. To be specific, the mean localization error of STI-WELM is at the same level with STI-ELM when only three APs are leveraged. However, as shown in Fig. 6, it reduces significantly when the required number of APs is between 4 and 6, and keeps the mean localization error at a low level when the number of APs is more than 7.

In summary, as long as no less than three APs are available in indoor environments, the STI-based localization approaches outperform RSS-based localization approaches. Furthermore, STI-WELM, which integrates the advantages of both STI and WELM, can overcome the heterogeneity issue of mobile devices for indoor localization and provide high localization

accuracy consistently even only a few APs are available in indoor environments.

D. Implementation of the Proposed IPS for Real Location-based Service

Since both the theoretical and experimental analysis have verified the superiority of the proposed IPS in terms of accuracy and robustness, we have implemented our IPS in the following four different indoor environments: Internet of Things Lab ($600m^2$) in Nanyang Technological University (NTU), Lecture Theater 22 ($500m^2$) in NTU, the Center for Berkeley Education Alliance for Research in Singapore (BEARS) headquarter ($1500m^2$), and the Center for Research in Energy Systems Transformation (CREST) Lab ($400m^2$) in University of California, Berkeley. It turns out that our system is able to provide satisfactory LBS across heterogeneous devices in these places, including indoor positioning, indoor navigation, real-time occupancy distribution monitoring and indoor geo-fencing, and has been fully operational for more than one year. For instance, [44] provides a video demo about our indoor navigation service on Google Glass, which is the mobile device (distinct from the reference device: iPad) to be localized. As shown in the video, by leveraging our proposed STI-WELM localization algorithm, our IPS offers high localization accuracy and seamless indoor navigation across heterogeneous devices.

VI. Conclusion

In this paper, we presented a robust and precise IPS by introducing STI, which is a new type of fingerprints and embodies more reliable and robust location signatures compared to traditional location fingerprints in the presence of heterogeneous devices and changing indoor environments. We also proposed a novel weighting scheme by taking into consideration of the relative importance of each RSS sample according to its corresponding STI value, for the WELM training process. On these grounds, we proposed the STI-WELM scheme which inherits the advantages of both STI and WELM. According to our experimental results, the STI-WELM scheme enhances the precision of indoor positioning by 39.89% over RSS-ELM, 33.54% over SSD-ELM and 11.45% over STI-ELM, respectively, which confirms the superiority of the STI approach to the traditional RSS fingerprints as well as the recently developed SSD approach. In addition, our IPS has been deployed in various types of indoor environments, such as lab, office space and lecture theater, and turns out to provide satisfactory LBS.

References

[1] B. Buchli, F. Sutton, and J. Beutel, *GPS-equipped wireless sensor network node for high-accuracy positioning applications*, pp. 179–195. Springer, 2012.

[2] H. Liu, H. Darabi, P. Banerjee, and J. Liu, "Survey of wireless indoor positioning techniques and systems," *Systems, Man, and Cybernetics, Part C: Applications and Reviews, IEEE Transactions on*, vol. 37, no. 6, pp. 1067–1080, 2007.

[3] Y. Gu, A. Lo, and I. Niemegeers, "A survey of indoor positioning systems for wireless personal networks," *Communications Surveys & Tutorials, IEEE*, vol. 11, no. 1, pp. 13–32, 2009.

[4] G. Deak, K. Curran, and J. Condell, "A survey of active and passive indoor localisation systems," *Computer Communications*, 2012.

[5] H. Zou, L. Xie, Q.-S. Jia, and H. Wang, "Platform and algorithm development for a rfid-based indoor positioning system," *Unmanned Systems*, vol. 2, no. 03, pp. 279–291, 2014.

[6] P. Bahl and V. N. Padmanabhan, "Radar: An in-building rf-based user location and tracking system," in *INFOCOM 2000. Nineteenth Annual Joint Conference of the IEEE Computer and Communications Societies. Proceedings. IEEE*, vol. 2, pp. 775–784, Ieee.

[7] M. Youssef and A. Agrawala, "The horus wlan location determination system," in *Proceedings of the 3rd international conference on Mobile systems, applications, and services*, pp. 205–218, ACM.

[8] S.-H. Fang, T.-N. Lin, and K.-C. Lee, "A novel algorithm for multipath fingerprinting in indoor wlan environments," *Wireless Communications, IEEE Transactions on*, vol. 7, no. 9, pp. 3579–3588, 2008.

[9] S.-H. Fang, Y.-T. Hsu, and W.-H. Kuo, "Dynamic fingerprinting combination for improved mobile localization," *Wireless Communications, IEEE Transactions on*, vol. 10, no. 12, pp. 4018–4022, 2011.

[10] A. Mahtab Hossain, Y. Jin, W.-S. Soh, and H. N. Van, "Ssd: A robust rf location fingerprint addressing mobile devices' heterogeneity," *Mobile Computing, IEEE Transactions on*, vol. 12, no. 1, pp. 65–77, 2013.

[11] J.-g. Park, D. Curtis, S. Teller, and J. Ledlie, "Implications of device diversity for organic localization," in *INFOCOM, 2011 Proceedings IEEE*, pp. 3182–3190, IEEE.

[12] S.-H. Fang, C.-H. Wang, S.-M. Chiou, and P. Lin, "Calibration-free approaches for robust wi-fi positioning against device diversity: a performance comparison," in *Vehicular Technology Conference (VTC Spring), 2012 IEEE 75th*, pp. 1–5, IEEE.

[13] C. Figuera, J. L. Rojo-lvarez, I. Mora-Jimnez, A. Guerrero-Curieses, M. Wilby, and J. Ramos-Lpez, "Time-space sampling and mobile device calibration for wifi indoor location systems," *Mobile Computing, IEEE Transactions on*, vol. 10, no. 7, pp. 913–926, 2011.

[14] A. Haeberlen, E. Flannery, A. M. Ladd, A. Rudys, D. S. Wallach, and L. E. Kavraki, "Practical robust localization over large-scale 802.11 wireless networks," in *Proceedings of the 10th annual international conference on Mobile computing and networking*, pp. 70–84, ACM.

[15] M. B. Kjrgaard, "Indoor location fingerprinting with heterogeneous clients," *Pervasive and Mobile Computing*, vol. 7, no. 1, pp. 31–43, 2011.

[16] F. Della Rosa, H. Leppakoski, S. Biancullo, and J. Nurmi, "Ad-hoc networks aiding indoor calibrations of heterogeneous devices for fingerprinting applications," in *Indoor Positioning and Indoor Navigation (IPIN), 2010 International Conference on*, pp. 1–6, IEEE.

[17] A. W. Tsui, Y.-H. Chuang, and H.-H. Chu, "Unsupervised learning for solving rss hardware variance problem in wifi localization," *Mobile Networks and Applications*, vol. 14, no. 5, pp. 677–691, 2009.

[18] F. Dong, Y. Chen, J. Liu, Q. Ning, and S. Piao, *A calibration-free localization solution for handling signal strength variance*, pp. 79–90. Springer, 2009.

[19] H. Wang, S. Sen, A. Elgohary, M. Farid, M. Youssef, and R. R. Choudhury, "No need to war-drive: unsupervised indoor localization," in *Proceedings of the 10th international conference on Mobile systems, applications, and services*, pp. 197–210, ACM.

[20] A. Rai, K. K. Chintalapudi, V. N. Padmanabhan, and R. Sen, "Zee: zero-effort crowdsourcing for indoor localization," in *Proceedings of the 18th annual international conference on Mobile computing and networking*, pp. 293–304, ACM.

[21] Y. Jiang, X. Pan, K. Li, Q. Lv, R. P. Dick, M. Hannigan, and L. Shang, "Ariel: Automatic wi-fi based room fingerprinting for indoor localization," in *Proceedings of the 2012 ACM Conference on Ubiquitous Computing*, pp. 441–450, ACM.

[22] V. Radu and M. K. Marina, "Himloc: Indoor smartphone localization via activity aware pedestrian dead reckoning with selective crowdsourced wifi fingerprinting," in *Indoor Positioning and Indoor Navigation (IPIN), 2013 International Conference on*, pp. 1–10, IEEE.

[23] C. Laoudias, D. Zeinalipour-Yazti, and C. G. Panayiotou, "Crowdsourced indoor localization for diverse devices through radiomap fusion," in *Indoor Positioning and Indoor Navigation (IPIN), 2013 International Conference on*, pp. 1–7, IEEE.

[24] J. C. Gower, "Generalized procrustes analysis," *Psychometrika*, vol. 40, no. 1, pp. 33–51, 1975.

[25] L. M. Ni, Y. Liu, Y. C. Lau, and A. P. Patil, "Landmarc: indoor location sensing using active rfid," *Wireless networks*, vol. 10, no. 6, pp. 701–710, 2004.

[26] G.-B. Huang, Q.-Y. Zhu, and C.-K. Siew, "Extreme learning machine: theory and applications," *Neurocomputing*, vol. 70, no. 1, pp. 489–501, 2006.

[27] G.-B. Huang, H. Zhou, X. Ding, and R. Zhang, "Extreme learning machine for regression and multiclass classification," *Systems, Man, and Cybernetics, Part B: Cybernetics, IEEE Transactions on*, vol. 42, no. 2, pp. 513–529, 2012.

[28] W. Zong, G.-B. Huang, and Y. Chen, "Weighted extreme learning machine for imbalance learning," *Neurocomputing*, vol. 101, pp. 229–242, 2013.

[29] M. Brunato and R. Battiti, "Statistical learning theory for location fingerprinting in wireless lans," *Computer Networks*, vol. 47, no. 6, pp. 825–845, 2005.

[30] E. A. Martnez, R. Cruz, and J. Favela, *Estimating user location in a WLAN using backpropagation neural networks*, pp. 737–746. Springer, 2004.

[31] Z.-l. Wu, C.-h. Li, J.-Y. Ng, and K. Leung, "Location estimation via support vector regression," *Mobile Computing, IEEE Transactions on*, vol. 6, no. 3, pp. 311–321, 2007.

[32] C. Feng, W. S. A. Au, S. Valaee, and Z. Tan, "Received-signal-strength-based indoor positioning using compressive sensing," *Mobile Computing, IEEE Transactions on*, vol. 11, no. 12, pp. 1983–1993, 2012.

[33] C.-t. Huang, C.-h. Wu, Y.-N. Yao-Nan Lee, and J.-T. Chen, "A novel indoor rss-based position location algorithm using factor graphs," *Wireless Communications, IEEE Transactions on*, vol. 8, no. 6, pp. 3050–3058, 2009.

[34] A. Kushki, K. N. Plataniotis, and A. N. Venetsanopoulos, "Kernel-based positioning in wireless local area networks," *Mobile Computing, IEEE Transactions on*, vol. 6, no. 6, pp. 689–705, 2007.

[35] Y. Jin, W.-S. Soh, and W.-C. Wong, "Indoor localization with channel impulse response based fingerprint and nonparametric regression," *Wireless Communications, IEEE Transactions on*, vol. 9, no. 3, pp. 1120–1127, 2010.

[36] H. Zou, L. Xie, Q.-S. Jia, and H. Wang, "An integrative weighted path loss and extreme learning machine approach to rfid based indoor positioning," in *4th IEEE International Conference on Indoor Positioning and Indoor Navigation (IPIN 2013)*, IEEE.

[37] H. Zou, X. Lu, H. Jiang, and L. Xie, "A fast and precise indoor localization algorithm based on an online sequential extreme learning machine," *Sensors*, vol. 15, no. 1, pp. 1804–1824, 2015.

[38] H. Cheng, F. Wang, R. Tao, H. Luo, and F. Zhao, "Clustering algorithms research for device-clustering localization," in *Indoor Positioning and Indoor Navigation (IPIN), 2012 International Conference on*, pp. 1–7, IEEE.

[39] M. B. Kjrgaard and C. V. Munk, "Hyperbolic location fingerprinting: A calibration-free solution for handling differences in signal strength (concise contribution)," in *Pervasive Computing and Communications, 2008. PerCom 2008. Sixth Annual IEEE International Conference on*, pp. 110–116, IEEE.

[40] S. L. Jackson, *Research methods and statistics: A critical thinking approach*. CengageBrain. com, 2011.

[41] T. S. Rappaport, *Wireless communications: principles and practice*, vol. 2. prentice hall PTR New Jersey, 1996.

[42] A. E. Hoerl and R. W. Kennard, "Ridge regression: Biased estimation for nonorthogonal problems," *Technometrics*, vol. 12, no. 1, pp. 55–67, 1970.

[43] K. Kaemarungsi and P. Krishnamurthy, "Analysis of wlans received signal strength indication for indoor location fingerprinting," *Pervasive and mobile computing*, vol. 8, no. 2, pp. 292–316, 2012.

[44] H. Zou, "Indoor navigation on google glass." https://www.youtube.com/watch?v=vJ4kJu4ivdE.

APPENDIX A
DERIVING (6)

Regarding $\widehat{RDS}$, we define

$$\widehat{RDS} = [P_1^R - \overline{RDS}, P_2^R - \overline{RDS}, ..., P_n^R - \overline{RDS}]/\hat{\sigma}, \quad (23)$$

where

$$\overline{RDS} = \sum_{i=1}^{n} P_i^R, \quad (24)$$

$$\hat{\sigma}^R = \sqrt{\frac{1}{n}\sum_{i=1}^{n}(P_i^R - \overline{RDS})^2}. \quad (25)$$

Then, we can have

$$\begin{aligned}
&\|\widehat{TDS} - \widehat{RDS}\|^2 \\
=& \sum_{j=1}^{n}\left(\frac{P_j - \overline{TDS}}{\hat{\sigma}} - \frac{P_j^R - \overline{RDS}}{\hat{\sigma}^R}\right)^2 \\
=& \sum_{j=1}^{n}\left(\frac{P_j - \overline{TDS}}{\sqrt{\frac{1}{n}\sum_{i=1}^{n}(P_i - \overline{TDS})^2}} - \frac{P_j^R - \overline{RDS}}{\sqrt{\frac{1}{n}\sum_{i=1}^{n}(P_i^R - \overline{RDS})^2}}\right)^2 \\
=& \sum_{j=1}^{n}\left(\frac{(P_j - \overline{TDS})^2}{\frac{1}{n}\sum_{i=1}^{n}(P_i - \overline{TDS})^2} + \frac{(P_j^R - \overline{RDS})^2}{\frac{1}{n}\sum_{i=1}^{n}(P_i^R - \overline{RDS})^2}\right. \\
&\left. - \frac{2(P_j - \overline{TDS})(P_j^R - \overline{RDS})}{\sqrt{\frac{1}{n}\sum_{i=1}^{n}(P_i - \overline{TDS})^2}\sqrt{\frac{1}{n}\sum_{i=1}^{n}(P_i^R - \overline{RDS})^2}}\right) \\
=& \frac{\sum_{j=1}^{n}(P_j - \overline{TDS})^2}{\frac{1}{n}\sum_{i=1}^{n}(P_i - \overline{TDS})^2} + \frac{\sum_{j=1}^{n}(P_j^R - \overline{RDS})^2}{\frac{1}{n}\sum_{i=1}^{n}(P_i^R - \overline{RDS})^2} \\
&- \frac{2\sum_{j=1}^{n}(P_j - \overline{TDS})(P_j^R - \overline{RDS})}{\sqrt{\frac{1}{n}\sum_{i=1}^{n}(P_i - \overline{TDS})^2}\sqrt{\frac{1}{n}\sum_{i=1}^{n}(P_i^R - \overline{RDS})^2}} \\
=& 2n - \frac{2n\sum_{j=1}^{n}(P_j - \overline{TDS})(P_j^R - \overline{RDS})}{\sqrt{\sum_{i=1}^{n}(P_i - \overline{TDS})^2}\sqrt{\sum_{i=1}^{n}(P_i^R - \overline{RDS})^2}} \\
=& 2n(1-\rho)
\end{aligned}$$

Han Zou received the B.Eng. (First Class Honors) from Nanyang Technological University, Singapore in 2012, where he is currently pursuing the Ph.D. degree in the School of Electrical and Electronic Engineering. He is also a Graduate Student Researcher with Berkeley Education Alliance for Research in Singapore Limited (BEARS). His research interests include mobile computing, Internet of Things, wireless sensor networks, indoor positioning and navigation systems, and indoor human activity sensing and inference.

Baoqi Huang obtained the B.E. degree in computer science from Inner Mongolia University (IMU), Hohhot, China, in 2002, the M.S. degree in computer science from Peking University, Beijing, China, in 2005, and the Ph.D. degree in information engineering from the Australian National University, Canberra, Australia, in 2012. From May 2013 to April 2014, he worked as a Research Fellow in Nanyang Technological University. He is with the College of Computer Science, IMU, where he is currently a professor. He was a recipient of the Chinese Government Award for Outstanding Chinese Students Abroad in 2011. His research interests include source localization, wireless sensor networks, and mobile computing.

Xiaoxuan Lu received his B.E. degree in Automation Engineering from Nanjing University of Aeronautics and Astronautics, China in 2013, and the M.E. degree in Electrical and Electronic Engineering from Nanyang Technological University, Singapore in 2015. He is currently pursuing the Ph.D. degree in Computer Science at University of Oxford, United Kingdom. His research interests focus on Internet of Things and machine learning techniques for sensor networks.

Hao Jiang obtained the B.E and Ph.D. degrees from the School of Information Science and Engineering, Xiamen University, China, in 2008 and 2013, respectively. He is currently engaged in postdoctoral research at the School of Electrical & Electronic Engineering, Nanyang Technological University, Singapore. His current research interests lie in localization system, sensor network, fiber optic sensor, and evolutionary algorithm.

Lihua Xie received the B.E. and M.E. degrees in electrical engineering from Nanjing University of Science and Technology in 1983 and 1986, respectively, and the Ph.D. degree in electrical engineering from the University of Newcastle, Australia, in 1992. Since 1992, he has been with the School of Electrical and Electronic Engineering, Nanyang Technological University, Singapore, where he is currently a professor and served as the Head of Division of Control and Instrumentation from July 2011 to June 2014. He held teaching appointments in the Department of Automatic Control, Nanjing University of Science and Technology from 1986 to 1989 and Changjiang Visiting Professorship with South China University of Technology from 2006 to 2011.

Dr Xie's research interests include robust control and estimation, networked control systems, multi-agent networks, and unmanned systems. He has served as an editor of IET Book Series in Control and an Associate Editor of a number of journals including IEEE Transactions on Automatic Control, Automatica, IEEE Transactions on Control Systems Technology, and IEEE Transactions on Circuits and Systems-II. Dr Xie is a Fellow of IEEE and Fellow of IFAC.